

## Development of tropical cyclones in the Indian Seas as revealed by satellite radiation and television data

D. R. SIKKA

*Institute of Tropical Meteorology, Poona*

**ABSTRACT.** Nimbus-II Medium Resolution Infra-red Radiometer (MRIR) and High Resolution Infra-red Radiometer (HRIR) data in combination with ESSA-I television photography is utilised to study the development of a deep depression in the Bay of Bengal during 14 to 17 June 1966. Development of a tropical cyclone in the Bay of Bengal and the Arabian Sea during November 1966 is also followed with the HRIR data and ESSA-3 television pictures. The results of the study show the usefulness of radiation data in determining the extent of the cirrus canopy and its location and determination of the general magnitude of the peripheral subsidence.

### 1. Introduction

Research work done by several workers utilising satellite data in the tropics have demonstrated that the most important operational use of satellite data in these areas is in the detection, tracking and determination of intensity changes of the tropical cyclones. Case studies of the tropical cyclone genesis in the north Indian Ocean using satellite television photographs have been reported by Koteswaram (1961), Sadler (1961), Kulshrestha and Gupta (1966), Rama Rao, Ramanathan and Srinivasan (1967), Sivaramakrishnan (1965) and Mukherjee and Mishra (1968) etc. These studies have revealed more or less similar features in the photographs depicting the various stages in the development of tropical cyclones in this area as in the case of hurricanes and typhoons of the North Atlantic and the West Pacific region studied by several American research workers. Tiros and Nimbus infra-red radiation data have also been used for the study of hurricanes and typhoons development by Bandeen *et al.* (1933), Allison and Thompson (1966), Warnecke *et al.* (1968) and Beran *et al.* (1968). The present study uses Nimbus II infra-red data along with the ESSA-I and ESSA-III television data to study the development of a monsoon depression in the Bay of Bengal and a severe tropical cyclone in the Bay of Bengal and its rejuvenation in the Arabian Sea.

### 2. Method of analysis

The cases selected are (i) the monsoon depression during the period 14-17 June 1966 and the severe tropical cyclone during the period 30 October to 13 November 1966. The synoptic weather charts for all

the standard isobaric levels for the above periods were prepared. Nimbus II Medium Resolution Infrared Radiometer (MRIR) digital maps and the photo prints for Channel I ( $6.4-6.9 \mu$ ) and Channel II ( $10-11 \mu$ ) together with the night time high Resolution Infra-red Radiometer (HRIR) ( $3.5-4.2 \mu$ ) digital maps and photo-prints of the monsoon depression case and the HRIR digital maps and photo prints for the severe tropical cyclone case have been used in the study together with the television pictures of ESSA-I and ESSA-III for the respective cases. Radiation data were obtained from the National Aeronautics and Space Administration (NASA) and the television pictures from the National Environmental Satellite Centre (NESC), Washington D.C. APT pictures available with the India Meteorological Department have also been used for the severe tropical cyclone case. Interpretation of satellite radiometric measurements is based on an equation of radiative transfer through the atmosphere and details of the method are available in Nimbus II users Guide. The radiance measured in Channel II is assumed to be directly proportional to the emitting temperature of the underlying surface or cloud tops, although the spectral interval  $10-11 \mu$  does not constitute a perfect window nor do natural surfaces radiate as black bodies. In the spectral region of Channel I as discussed by Bandeen *et al.* (1963) only radiation emitted from the water vapour of the upper troposphere and stratosphere can penetrate to the satellite. Therefore equivalent black body temperatures ( $T_{BB}$ ) determined from the measured radiation fluxes are representative of the mean temperature and water vapour content of these

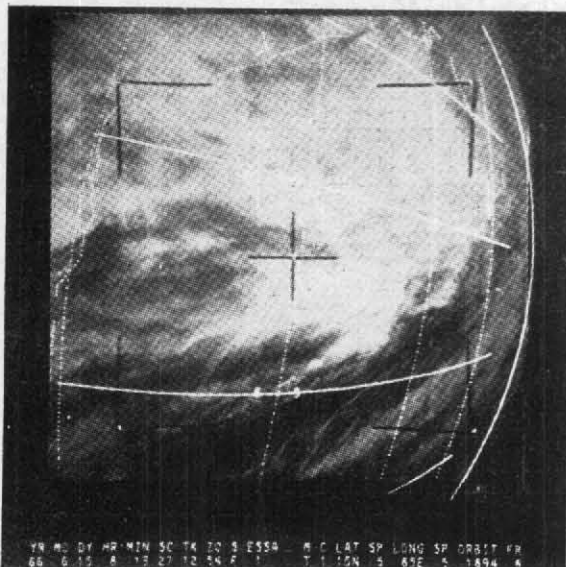


Fig. 1

ESSA I photograph of the tropical disturbance in the Bay of Bengal at 0813 GMT on 15 June 1966. Orbit : 1894 j

emitting layers. However, difficulties arise in the interpretation of Channel I data in the presence of cirrus and multilayered clouds which are always present during the development of tropical storms. Study by Beran *et al.* (1968) using Nimbus II MRIR data has shown that although it is difficult to establish a specific  $T_{BB}$  which delineates cloud free from cloud contaminated data, it is very probable that  $T_{BB}$  greater than  $240^{\circ}\text{A}$  are free from significant cloud contamination and  $T_{BB}$  less than  $235^{\circ}\text{A}$  are contaminated by multilayered clouds. Thus at temperatures lower than  $235^{\circ}\text{A}$ , the information content of Channel I is redundant when concurrent Channel II data are available. HRIR ( $3.5 - 4.2 \mu$ ) window is much cleaner than Channel II window from water vapour absorption but the information content is considered to be not very reliable below  $230^{\circ}\text{A}$  because they are at the lower limits of detection of the radiometer. The accuracy of the measured temperatures by Nimbus II satellite radiometers varies from about  $2-5^{\circ}\text{A}$  due to atmospheric attenuation by water vapour and carbon dioxide. The effective radiation heights, *i.e.*, the height where the ambient temperature equals the equivalent black body temperature, were determined for all days for the central region of the disturbances under study from the mean radiosonde data of the Indian stations. Due to the limitations in the accuracy of Nimbus II and radiosonde data the effective radiation heights may differ by about 1 km.

Infra-red pictorial data is obtained at NASA from the original analogue records and the picture

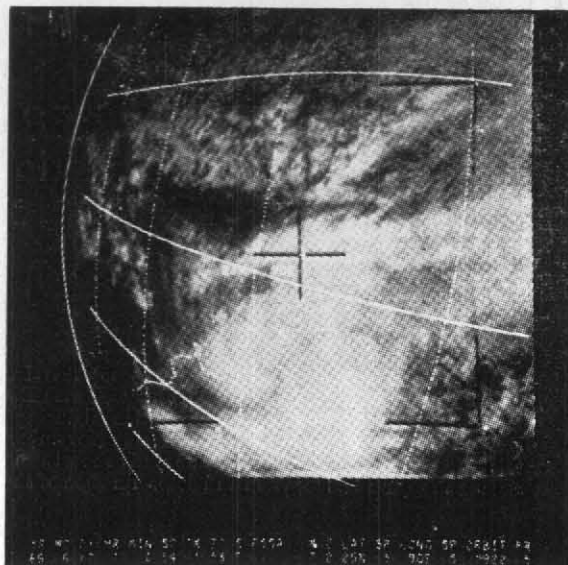


Fig. 2

ESSA I photograph of deep depression in the north Bay of Bengal at 0707 GMT on 17 June 1966. Orbit : 1922

does not depict clouds but only temperatures and therefore different grey scales correspond to different ranges of temperatures. The very white regions would represent very cool tops in the central overcast of the tropical disturbance.

In the following discussions on the cases under study only typical diagrams are shown.

### 3. Discussion of case studies

#### 3.1. Case I—Monsoon Depression of 14-17 June 1966

The northern limit of monsoon over peninsular India and west coast was about  $20^{\circ}\text{N}$  on 12 June. On 13 June ESSA-I pass over the Bay of Bengal showed a blob of cloud over central Bay and the region from coastal Andhra Pradesh towards this blob was heavily clouded. On 14 June whereas the central region of the blob over central Bay was near  $15^{\circ}\text{N}$ ,  $88^{\circ}\text{E}$  another patch of cloud was seen over SE Bay of Bengal. On 15 June a low pressure area formed in the central Bay of Bengal and the associated cloudiness as photographed by ESSA-I during its orbit number 1894 (0813 GMT) is shown in Fig. 1. This low pressure area intensified into a depression on the night of 15-16 June. It deepened further on 16 June. Fig. 2 shows ESSA-I photograph of the situation on 17 June at 0707 GMT. The picture clearly shows banded structure, the central overcast in its formative stage and even a wedge of clear area to the west of this overcast. Cirrus outflow is also observed in the northwestern sector. The

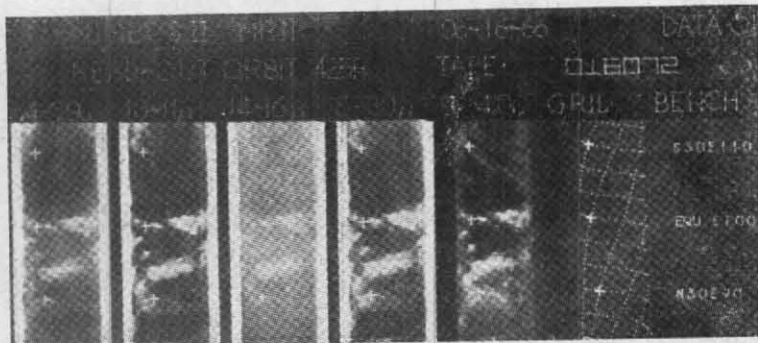


Fig. 3

Photoprint of Nimbus II MRIR data at 0530Z on 16 June 1966, Orbit: 425

centre of the circulation is very near the central overcast and lies near  $21^{\circ}\text{N}$ ,  $90^{\circ}\text{E}$ . Thus from the satellite photograph the inferred intensity of system is one of deep depression (wind speed 28–33 kt) but very near to the tropical cyclone stage (wind speed 35–47 kt). The disturbance weakened over East Pakistan on 18 June.

Fig. 3 shows the photoprint of Nimbus II MRIR on 16 June (0530 GMT). The system is seen in all the channels as a region of low radiation values indicating that the cloud tops had reached high in the troposphere. Low radiation values are oriented towards SW from the central region of the depression. There is another E-W oriented patch of low radiation values in the equatorial region. The digital data of Channel II (Fig. 4) showed  $T_{BB}$  values of about  $210^{\circ}\text{A}$  in the central region of the disturbance on the night of 16 June with inferred cloud top height being about 14 km. Channel I also showed very low  $T_{BB}$  values in the central region due to the presence of heavy multilayered clouding. Similar features were observed in the MRIR pictorial data on 15 June also.

The area covered by low radiation values of  $220^{\circ}\text{A}$  had increased from 14 to 16 June. Significant difference was noticed in the  $T_{BB}$  values in Channel I on 16 June when the region to the NW of the centre was considerably warmer ( $>240^{\circ}\text{A}$ ) in comparison to the NE sector ( $<230^{\circ}\text{A}$ ). This indicated that in the upper troposphere descent was taking place to the NW of the disturbance which also lay to the east of the upper tropospheric ridge. However, it is very difficult to get support of this descent in the upper troposphere from the radiosonde data of Calcutta. Evidence of this descent is provided in Fig. 2 which shows either absence of clouds to the west of the depression or presence of low clouds. The night time HRIR digital data also showed low radiation values ( $T_{BB} < 230^{\circ}\text{A}$ ) in the region of the depression and

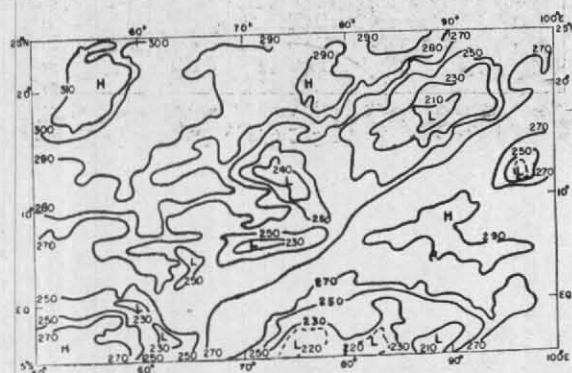


Fig. 4

Nimbus II Channel II radiation analysis ( $^{\circ}\text{A}$ ) indicating deep depression near  $20^{\circ}\text{N}$ ,  $90^{\circ}\text{E}$  at 0553Z on 16 June 1966. Orbit: 424-425

the area covered by these low radiation values had increased from 14 to 16 June. Fig. 5 (a) shows the mapping of these HRIR radiation values in the area of the disturbance on the night of 16–17 June. Fig. 5(b) shows the corresponding photoprint of the HRIR data. Fig. 6 shows Channel II mapping on 17 June when the disturbances was in its maximum intensity.

Thus the satellite radiation data showed that the deep depression which formed on 16 June developed to the east of the descending air in the upper troposphere as indicated by Channel I information. It was also observed that there was an increase in the area covered by low radiation values from 14 to 17 June and the cloud tops in the central region of the disturbance reached about 14 km in height.

### 3.2. Case II—Bay of Bengal and Arabian Sea tropical cyclone of 30 October to 13 November 1966

On 28 October 1966 the surface anticyclone over China had intensified and its southern edge

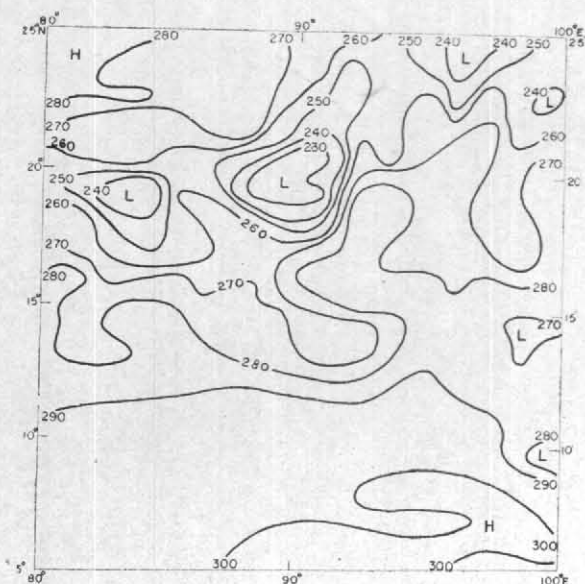


Fig. 5 (a)

Nimbus II HRIR radiation analysis ( $^{\circ}\text{A}$ ) of the deep depression at 1653Z on 16 June 1966

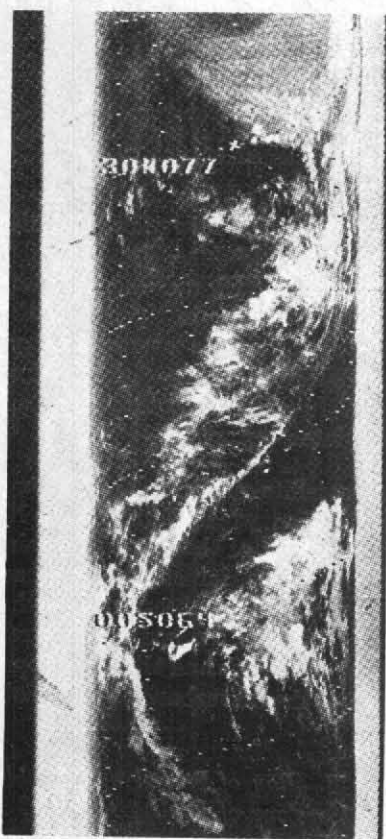


Fig. 5 (b)

Photoprint of Nimbus II HRIR data from Orbit 431-432 at 1655 Z on 16 June 1966 showing deep depression in the north Bay of Bengal

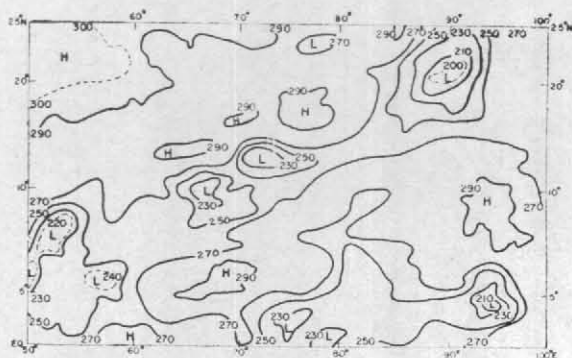


Fig. 6

Nimbus II Channel II radiation analysis ( $^{\circ}\text{A}$ ) at 0508Z on 17 June 1966, Orbit 438

had approached towards north Vietnam. As a result NE trades strengthened over the south China Sea. The equatorial trough was south of its normal position in the Arabian Sea, Bay of Bengal and the Western Pacific region and its axis at 700 mb ran along  $5^{\circ}$ – $7^{\circ}\text{N}$ . Lower tropospheric equatorial westerlies strengthened and Gan Island reported 20–25 kt winds at 850 and 700 mb between 29 to 31 October. Equatorial cloudiness very much increased and an E-W oriented ITCZ type cloud band was continuously oriented between the equator and  $5^{\circ}\text{N}$  from  $50^{\circ}\text{E}$  to  $110^{\circ}\text{E}$ . It is within this equatorial cloudiness that a circular area was found to develop near  $8^{\circ}\text{N}$ ,  $100^{\circ}\text{E}$  on 30 October as shown in Fig. 7.

Corresponding 700 mb chart for 30 October (1200 GMT) is shown in Fig. 8 depicting the marked activity of the troughs on either side of the equator with cyclonic vortices embedded in each of them. HRIR digital data on the night of 30–31 October showed small area of low radiation values ( $< 235^{\circ}\text{A}$ ) in the vicinity of the cyclonic circulation in the Gulf of Siam region and higher temperatures to the western side of the disturbance. However, due to the averaging process in the preparation of grid point map for HRIR observations no structural detail of this cloud cluster could be seen. The disturbance intensified into deep depression on 31 October and lay near  $10^{\circ}\text{N}$ ,  $96^{\circ}\text{E}$  at 1200 GMT. ESSA III photograph on this day showed the characteristic comma shaped cloudiness with the overcast to the southwest of the centre and a link up with the heavy clouding in the near equatorial zone. HRIR photoprint as well as digital data showed that the disturbance had organised further and cirrus had developed a canopy of about 2 degrees in diameter. The area covered by the cold spot of  $T_{LB}$  value  $< 235^{\circ}\text{A}$  was found to have further enlarged. About 15 hours later ESSA III satellite photograph on 1 November indicated that the disturbance had developed into a tropical

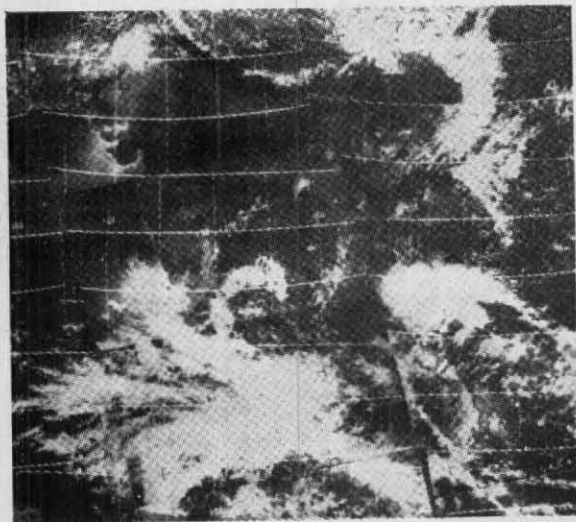


Fig. 7

ESSA III mosaic of the incipient stage of the tropical disturbance near  $8^{\circ}\text{N}$ ,  $100^{\circ}\text{E}$  from Orbits 348-350 on 30 October 1966

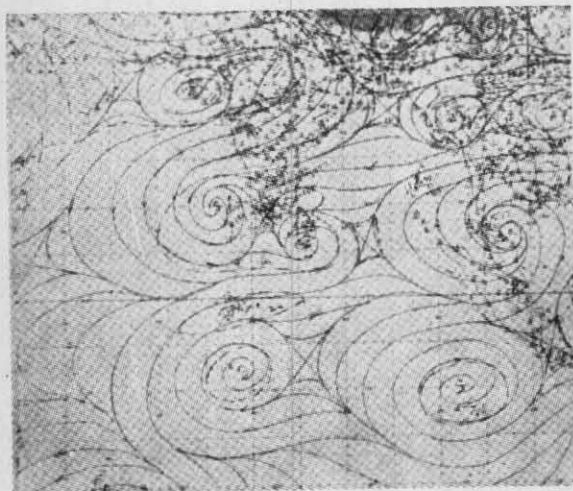


Fig. 8

700mb streamlines isotach chart at 12 GMT on 30 October 1966

cyclone with central overcast of about 3 degrees diameter and cirrus outflow in the NW sector. Fig. 9 shows the photoprint of HRIR observation on the night of 1 November. Characteristic cirrus outflow bands are seen along Andhra coast. The storm further intensified and lay near  $11^{\circ}\text{N}$ ,  $85^{\circ}\text{E}$  at 12 GMT of 2 November and near  $13^{\circ}\text{N}$ ,  $81^{\circ}\text{E}$  at 00 GMT of 3 November. Fig. 10 shows the HRIR digital data view of the storm between these two synoptic hours at 1750 GMT of 2 November. The central region of the storm covered by  $T_{BB}$  values  $< 230^{\circ}\text{A}$  was considerably large. The temperatures sensed by HRIR radiometer to the SW of the storm region were about  $280^{\circ}\text{A}$  indicating much less cloudiness. The storm



Fig. 9

Photoprint of Nimbus II HRIR data from Orbit 2269 at 1636 Z on 1 November 1966 showing the tropical cyclone in the SW Bay of Bengal

at this stage had separated itself from the equatorial cloud band. The storm continued to intensify further till 3 November. Maximum wind estimated from ESSA III photograph on 3 November on the basis of the nomogram by Fritz *et al.* (1966) was over 100 kt. Ship S. S. *Rajula* passed very near the storm centre on this day and its log observation showed that it had experienced a maximum wind of 15 to 17 BF (94-114 kt) and its barogram recorded lowest pressure of 961 mb. Crossing coast on 3 November the storm weakened over Peninsula on 4 November. The cloud structure broke up on 4 November as seen in the satellite photograph and the organisation in the HRIR data was also found to decrease very much. The system emerged into

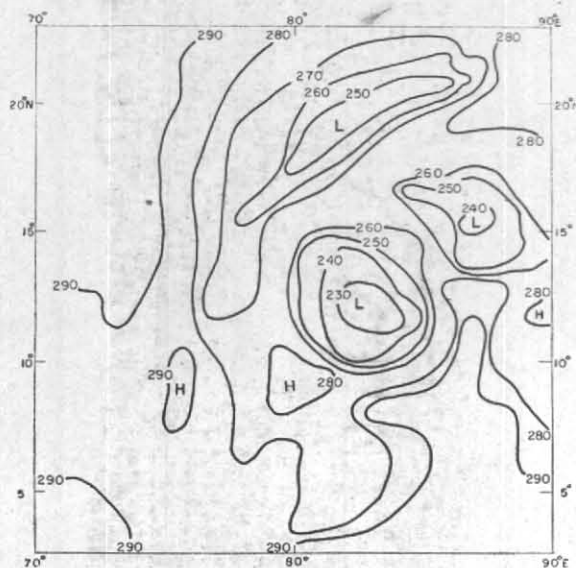


Fig. 10

Nimbus II HRIR radiation analysis ( $^{\circ}\text{A}$ ) from Orbit 2283 at 1750Z on 2 Nov 1966 showing the mature stage of tropical cyclone in the SW Bay of Bengal

the Arabian Sea on 5 November and reintensified into a severe tropical cyclone on 7 November. Fig. 11 shows ESSA III photograph on 8 November with a clear storm eye. HRIR data from 5 to 7 November again showed growing cirrus canopy and expansion as well as organisation of the area covered by  $T_{BB}$  values  $< 230^{\circ}\text{A}$ . Fig. 12 shows the HRIR photoprint of the storm on the night of 8-9 November when it had probably reached its maximum intensity. The eye of the storm as well as large cirrus canopy and details of outflow spirals are clearly seen. Digital data showed that in the region covered by cirrus canopy, the cloud tops were above 11-12 km ( $T_{BB} < 230^{\circ}\text{A}$ ). The storm continued to move NW without much loss of intensity till 11 November. On 10 November ship *Barboza* recorded lowest pressure of 965 mb. The ship M.V. *Nedar Weser* passed close to the centre of the storm on 11 November and its barogram showed a pressure of 969 mb. The storm weakened on the Arabian coastal region on 13 November. Pedgley (1969) has described the last phase of the storm's history. The storm weakened rather rapidly on approaching Arabian coast. Fig. 13 shows HRIR photoprint on the night of 11-12 November which stands in sharp contrast to Fig. 12 and is typical of the weakening phase of the storm.

The study of the complete series of HRIR data during the life history of the tropical cyclone from its incipient stage on 28 October to its most intense stage on 8 November and dissipation stage on 12 and 13 November showed that this form of

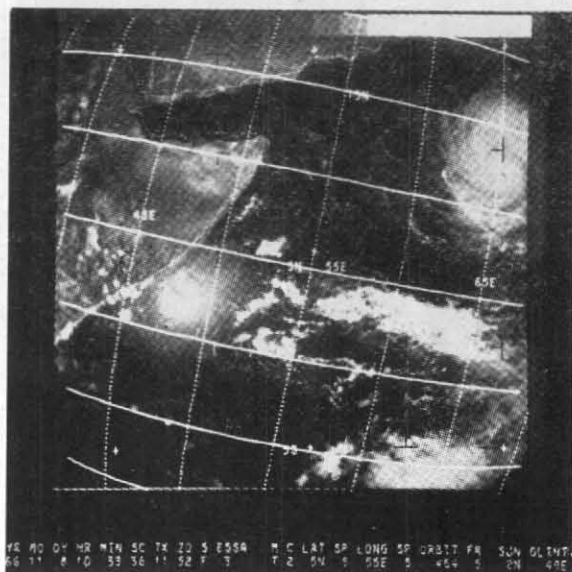


Fig. 11

ESSA III view of severe tropical cyclone (with eye) in the Arabian Sea at 1034Z on 8 Nov 1966, Orbit 464

data depicted the various stages of the storm very well. However, the size of the cirrus canopy in its mature stage was found to be smaller than in the television photographs of ESSA III. Such differences in the cirrus canopy between the television and HRIR photographs have been also reported by Hubert *et al.* (1969) in the case of Atlantic hurricanes.

### 3.3. Cirrus canopies in October-November 1966 tropical storm and updrafts within the clouds

The common features which were observed in the ESSA III television pictures and the HRIR photoprints during the mature stage of the tropical cyclone in the Bay of Bengal and in the Arabian Sea were (i) the bright disc of central overcast region or the cirrus canopy, (ii) the cloud rift in the southwestern sector of the storm and (iii) strong diffuse edges in the western and eastern peripheral regions of the storm between 7-10 November 1966 indicating strong peripheral subsidence. The canopy was found to dissipate when the storm started weakening. Wexler *et al.* (1966) have studied the cirrus canopies in several tropical storms and are of the view that the sharp edges would occur where the radial outflow becomes small and where the tangential velocity is at a relative maximum. Ramanathan (1971) has also studied the radial outflow from the satellite pictures of the storm under study and has obtained similar results. Time changes in the cirrus canopy at 24 hours interval have also been examined in this study for the period 1-3 November 1966 when the storm lay in the Bay of Bengal



Fig. 12

Photoprint of Nimbus II HRIR data Orbit 2363 at 1803 Z on 8 Nov 1966 showing the severe tropical cyclone in the Arabian Sea (with eye)

and also for the period 6–10 November during its history in the Arabian Sea. A tendency for increase in both the area as well as the symmetry of over all canopy patterns was observed during the intensification of the storm from 1–3 November and 6–8 November. Wexler *et al.* have observed that such changes in the canopy size of developing storms are indicative of the variation of area of active convection in the eye wall. It is believed that cirrus in the mature tropical storm is generated by the penetrative convection which is most common in the eye wall but may also occur in the spiral bands. Following their work and assuming continuity between the origin of cirrus from the cumulonimbus and the rate of increase of the cirrus volume in the steady state, the mean updraft at the base of the cirrus layer has been computed in the following way.

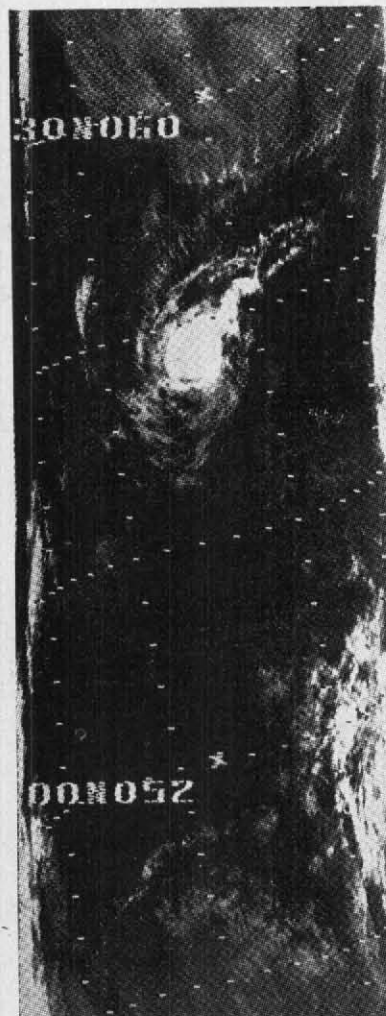


Fig. 13

Photoprint of Nimbus II HRIR data from Orbit 2403 at 1810 Z on 11 Nov 1966 showing the weakening phase of the tropical cyclone off Arabian Sea

$$AcW = H dA/dt \quad (1)$$

where,  $A_c$  is the area of penetrative cumulonimbus,  $W$  is the mean updraft at the base of the cirrus layer,  $H$  is the thickness of the cirrus layer and  $A$  is the horizontal area of the cirrus. The average rate of increase of area of the cirrus from the 24 hourly satellite photographs between 1–3 November and 6–8 November was found to be  $3.0 \times 10^4 \text{ km}^2/\text{hr}$ . The following figures have been used for other parameters of (1).

$$H = 2 \text{ km (assumed)}$$

$$A_c = 4 \text{ per cent of the total average area of the storm of } 350 \text{ km radius}$$

$$= 1.5 \times 10^4 \text{ km}^2/\text{hr.}$$

The computed value of the mean updraft ( $W$ ) over the entire area of cumulonimbus clouds is

the storm is found to be about  $1.1 \text{ m sec}^{-1}$ . Under the assumption of these calculations we find that about 4 per cent of the area of convection estimated after Malkus *et al.* (1961) and a mean updraft of about  $1 \text{ m sec}^{-1}$  was just enough for maintaining the cirrus canopy during the mature stage of the storm under study.

#### Acknowledgement

The author appreciates the help of World

Data Centre A, Rockets and Satellites, Goddard Space Flight Centre (NASA) Greenbelt, Maryland, U.S.A, for providing him with series of digital radiation maps and MRIR and HRIR photoprints used in the study. He also expresses his thanks to the National Environmental Satellite Centre (ESSA), Washington D.C., for supplying him with a number of satellite television pictures and mosaics used in the study.

#### REFERENCES

- Allison, L. J. and Thompson, H. P. 1967 "TIROS VII Infra-red radiation coverage of the 1963 Atlantic Hurricane season with supporting television and conventional meteorological data" NASA Tech. Rep., 48 pp.
- Bandeem, W. R., Conrath, B. J. and Hanel, R.A. 1963 *J. Atmos. Sci.*, **20**, pp. 609-614.
- Bandeem, W. R., Conrath, B. J., Nordberg, W. and Thompson, H. P. 1963 "A Radiation view of Hurricane Anna from TIROS III Meteorological Satellite" *Rocket and Satellite Meteorology*, North Holland Publ. Co., Amsterdam, pp. 224-233.
- Bran, D. W., Merritt, E. S. and Chang, D. T. 1968 "Interpretation of Baroclinic systems and wind fields as observed by Nimbus II MRIR", Final Rep., Cont. NAS-5-10334, 135 pp.
- Fritz, S., Hubert, L. F. and Timchalk, A. 1966 *Mon. Weath. Rev.*, **94**, pp. 231-236.
- Hubert, L. F., Timchalk, A. and Fritz, S. 1969 "Estimating maximum wind speed of Tropical Storms from high Resolution Infrared data", ESSA Tech. Rep., NESC, 50, 33 pp.
- Koteswaram, P. 1961 "Cloud Patterns in a Tropical cyclone in the Arabian Sea viewed by TIROS I Meteorological Satellite", Hawaii Inst. Geophys. Sci. Rep. 2, Cont. AF 19 (604) 6156, 34 pp.
- Kulshrestha, S. M. and Gupta, M. G. 1966 *J. appl. Met.* **5**, pp. 373-376.
- Malkus, J. S., Ronne, C. and Chaffe, M. 1961 *Tellus*, **13**, pp. 8-30.
- Mukherjee, A. K. and Mishra, R. K. 1968 *Indian J. Met. Geophys.*, **19**, pp. 295-304.
- Pedgley, D. E. 1969 *Weather*, **24**, pp. 456-468.
- Ram Rao, M., Ramanathan, A. S. and Srinivasan, V. 1967 *Indian J. Met. Geophys.*, **18**, pp. 485-490.
- Ramanathan, A. S. 1971 *Ibid.*, **22**, 3, pp. 325-330.
- Sivaramakrishnan, M. V. 1965 "Structure of Tropical Cyclones as revealed by TIROS cloud pictures taken over the Indian region". Proc. Symp. Met. Results of I.I.O.E., Bombay, July 1965. pp. 285-287.
- Warnecke, G., Allison, L. J., Kreins, E. R. and McMillin, L. M. 1968 "A Satellite view of Typhoon Marie, 1966 development", NASA Tech. Note TN-D-4757, 94 pp.
- Wexler, R., Merritt, E. S. and Chang, D. 1966 "Cirrus canopies in Tropical Storms". Final Rep. Cont. Cwb.-11305 prepared for NESC, Washington, 31 pp.

#### DISCUSSION

DR. D.M. PATEL : Is the formula  $A_c W = H \frac{dA}{dt}$  empirical ?

SHRI D.R. SIKKA : It is a simplified form of the continuity equation. It is assumed that the cirrus clouds originate in the penetrative cumulonimbus clouds and therefore the rate of production of cirrus volume is given by  $A_c W$  where  $A_c$  is the area of  $C_b$  clouds and  $W$  is the updraft. Assuming a steady state, the rate of increase of cirrus volume is given by the right hand side of the equation,  $H$  being the constant depth of the layer of the cirrus.

SHRI V. SRINIVASAN : How is  $dA/dt$  determined ?

SHRI SIKKA : The change of the elliptical area in 24 hr intervals has been determined from HRIR photoprints.